

Research Note

Spatial variability of compact extragalactic radiosources

M. Feissel^{1,2}, A.-M. Gontier¹, and T.M. Eubanks³

¹ Observatoire de Paris/CNRS UMR8630, 61 av. de l'Observatoire, 75014 Paris, France

² Institut Géographique National/LAREG, 8 Av. Blaise Pascal, Champs sur Marne, 77455 Marne la Vallée Cedex 2, France

³ US Naval Observatory, Washington, DC 20392, USA

Received 6 April 2000 / Accepted 18 May 2000

Abstract. Several hundreds of compact extragalactic radiosources (mainly quasars, but also BL Lac and galaxies) are monitored in a series of permanent VLBI geodetic and astrometric programs that were initiated in the late 1970's in support to the solar system exploration, for studying the Earth's rotation and crustal deformations, and for creating the celestial reference frame later recommended by the IAU as the International Celestial Reference Frame (ICRF). Time series of directions of ICRF objects can be established at a sub-milliarcsecond precision level. A subset of 16 objects with a dense observational history over 1988-1999 are studied in order to derive information on the geometric and statistical properties of their emission at centimetric wavelength.

Key words: astrometry – reference systems – galaxies: quasars: general

1. Introduction

VLBI monitoring of compact extragalactic radiosources started in the 1970's as a secondary objective of major projects such as the solar system exploration, the determination of plate tectonics and crustal deformations or the Earth's rotation and deformations (see Sovers et al. 1998 for a review of experiments, models and results in astrometry and geodesy with VLBI). The sets of accurate coordinates of the observed radiosources materialized the quasi-inertial reference frame to which the motions of interest were referred. The first sets of objects selected for these purposes were both bright and compact at S and X bands with the existing observing capabilities. The scientific interest in the celestial reference *per se* increased with the continuous progress of VLBI technology (hardware and software) and the progressive extension of the observing network to a worldwide one. The set of monitored sources grew from a few tens to currently over 600.

The complete data set (2.6 millions observations to date) is organized in 24-hour multi-baseline observing sessions in the S and X bands (corresponding to respective frequencies

Table 1. Physical characteristics of the 667 ICRF Ext-1 fiducial objects

| Type of object | % | Total flux (Jansky) | % | Redshift | % | Precision (μ as) | % |
|----------------|----|------------------------|----|----------|----|--------------------------|----|
| Quasars | 66 | 0-1 | 35 | 0-1 | 49 | < 0.5 | 56 |
| BL Lac | 11 | 1-2 | 41 | 1-2 | 34 | 0.5-1.0 | 20 |
| Galaxy | 8 | 2-4 | 17 | 2-3 | 13 | 1.0-2.0 | 11 |
| Other | 15 | > 4 | 7 | 3-4 | 4 | > 2.0 | 13 |

2.3 GHz and 8.4 GHz, and wavelengths 13 cm and 3.6 cm). It is periodically reanalyzed to take advantage of the progress in data analysis capabilities and in modelling of the complex set of phenomena that are to be dealt with for astro-geodetic research. These phenomena concern local and global atmospheric and oceanic effects, the influence of ice sheets or of the fluid core on the Earth's rotation, solid Earth and oceanic tides, plate tectonics, etc. The results used in this work are a part of the recent re-analysis for the ICRF, the so-called ICRF-Ext.1 (Ma et al. 1998; IERS 1999; <http://hpiers.obspm.fr/webiers/results/icrf/README.html>) which materializes the IAU-recommended International Celestial Reference System (ICRS) (see Feissel & Mignard 1998). Table 1 summarizes the general characteristics of the 667 sources in ICRF-Ext.1.

The radiosource coordinates in ICRF and ICRF-Ext.1 are derived from the complete set of observations over 1979-1999. They are qualified in two ways, 1. by ascribing realistic uncertainties that take into account both the random and systematic errors, and 2. by categorizing them, in decreasing order of confidence, as “defining”, “candidates”, and “other”. This complex assessment scheme reflects the existence of variabilities in the apparent directions of the sources, a nuisance for astrometry that may become a signal for astrophysics, if detailed information is available. This study is based on the estimation of session-per-session coordinates in a fixed reference frame for many sources of ICRF-Ext.1. We select sources with a strong observational history after 1988.0 – a time when the global astro-geodetic VLBI program reached a first maturity stage. We then study the source variability in a local frame related to the direction of maximum variance of the series of positions.

Send offprint requests to: M. Feissel (feissel@ensg.ign.fr)

Table 2. 16 radiosources continuously observed over 1988-1999

| Source | Other Name | Type of object | Redshift | Flux dens. at 6 cm (Jansky) | Spect class ¹ | Abs. Mag. | Nb of indiv values | Std. error (0.5a) $\alpha \cos \delta$ (μas) | δ (μas) |
|----------|------------|----------------|----------|-----------------------------|--------------------------|-----------|--------------------|-----------------------------------------------------------|-----------------------------|
| 0016+731 | | Quasar | 1.78 | 1.65 | | -26.6 | 402 | 142 | 168 |
| 0133+476 | DA55 | Quasar | 0.86 | 3.26 | HP | -24.9 | 295 | 40 | 36 |
| 0212+735 | | Quasar | 2.37 | 2.20 | HP | -26.5 | 1122 | 215 | 207 |
| 0234+285 | 4C28.07 | Quasar | 1.21 | 2.80 | HP | -26.2 | 881 | 60 | 104 |
| 0300+470 | 4C47.08 | BL Lac | | 2.22 | BL | | 662 | 132 | 85 |
| 0552+398 | OA198 | Quasar | 2.37 | 5.43 | | -28.5 | 2498 | 47 | 43 |
| 0851+202 | OJ287 | BL Lac | 0.31 | 2.61 | HP | -25.5 | 2232 | 102 | 63 |
| 0923+392 | 4C39.25 | Quasar | 0.70 | 7.57 | S1.0 | -25.3 | 2285 | 119 | 59 |
| 1156+295 | 4C29.45 | Quasar | 0.73 | 1.46 | HP | -28.6 | 385 | 76 | 157 |
| 1308+326 | AU CVn | Quasar | 1.00 | 1.50 | HP | -28.6 | 1144 | 119 | 114 |
| 1611+343 | DA406 | Quasar | 1.40 | 2.32 | | -27.6 | 904 | 42 | 101 |
| 1633+382 | 4C38.41 | Quasar | 1.81 | 4.08 | | -28.0 | 399 | 207 | 211 |
| 1637+574 | OS562 | Quasar | 0.75 | 1.75 | S1.2 | -26.4 | 156 | 133 | 165 |
| 1739+522 | 4C51.37 | Quasar | 1.38 | 1.99 | HP | -26.5 | 1136 | 65 | 90 |
| 1803+784 | | BL Lac | 0.68 | 2.63 | HP | -26.8 | 1695 | 69 | 82 |
| 2234+282 | CTD135 | Quasar | 0.80 | 1.06 | HP | -24.6 | 1385 | 260 | 185 |

¹ Spectral classification according to Véron & Véron (1998) [HP: High optical polarization (> 3%); S1.0, S2.0: Intermediate Seyfert galaxies; BL Confirmed BL Lac object.]

2. The astrometry data set

The astrometry data set used in this study is a time series of session-per-session source positions computed in a homogeneous reference frame from observations going back to August 1979.

For historical reasons, the numbers of observations per source are extremely uneven. Some sources that were used for providing reference directions in the early years of VLBI appeared to be too variable or too extended after some years and were discarded to the benefit of other, fainter sources that became usable for astrometric purposes thanks to the progress in technology. Some source considered as best fitting the astro-geodetic needs are repeatedly observed, while others, that are less useful for this purpose, are re-observed less frequently, mainly for astronomical studies.

According to Ma et al. (1998) there are two major causes for the current limitation in accuracy of source positions.

- The first cause is connected to the atmospheric delay correction combined with the geometry of the observing networks. The uncertainty in the modelling of the propagation delay due to the wet component of the troposphere, combined with deficiencies in the network geometry (majority of stations in the northern mid- latitudes, short N-S components of the baselines yielding to the observation of low declination objects at low elevation, where the mis-modelling of the delay has the largest effect), may give rise to systematic errors in declination at the level of 0.5 mas (milliarcsecond) in the zone around the equator.
- The second cause is related to the fact that no radiosource is really point-like when observed in centimetric wavelength with baseline lengths around 6000 km. If the source struc-

ture is extended or not circular, its apparent direction may change as a function of the length and orientation of the baselines. This effect should be minimized with the practice of running 24-hour sessions, during which the Earth's sidereal rotation leads to the diversification of the projections of the baselines on the source structure. Moreover, despite the selection of quiet objects for astro-geodetic work, any of them may exhibit changes in their emission structure that will make their apparent direction change with time. In principle it is possible to accurately correct this effect, provided that repeated maps of the sources are available (Charlot & Sovers, 1997). In the framework of the ICRF maintenance, a systematic mapping program is under way (Fey & Charlot 1997, 2000; <http://www.usno.navy.mil/RRFID>). However, the overall correction procedure is not yet implemented in the existing global analysis softwares. This mismodelling may propagate errors into the source positions at the level of 0.2 mas.

The latter effect is precisely the one we investigate in this study, based on the computed coordinates of the radiosources in a homogeneous reference frame, with one determination for each of the sessions in which the source was observed.

In order to be able to use standard time series statistics, the original series with irregular spacing is first transformed into equally spaced time series by performing weighted averages. Within the set of original sources, only those that could provide a continuous (or quasi-continuous) series of right ascensions and declinations at 6-month intervals over 1988-1999 are considered. In addition, in order to avoid the zone where declination instabilities due to inaccurate modelling of the tropospheric wet delay could mix with actual source instabilities,

Table 3. Equatorial direction and size of maximum standard deviation, and in the perpendicular direction

| Source | Other Name | Dir. (deg) | Std. dev., 0.5a interv. | | Structure index X S | | Date |
|----------|------------|------------|-------------------------|---------------------|---------------------|------------|------|
| | | | Max μas | Perp μas | | | |
| 0016+731 | | 124 | 191 | 116 | 2 1 | 13.10.1995 | |
| 0133+476 | DA55 | 30 | 46 | 28 | 2 2 | 23.04.1996 | |
| | | | | | 2 1 | 10.01.1997 | |
| 0212+735 | | 160 | 220 | 198 | 2 2 | 08.07.1994 | |
| 0234+285 | 4C28.07 | 64 | 97 | 56 | 3 2 | 08.07.1994 | |
| 0300+470 | 4C47.08 | 2 | 132 | 84 | 2 1 | 08.07.1994 | |
| 0552+398 | OA198 | 128 | 54 | 55 | 2 1 | 13.10.1995 | |
| 0851+202 | OJ287 | 118 | 67 | 98 | 2 1 | 13.10.1995 | |
| 0923+392 | 4C39.25 | 126 | 40 | 132 | 2 1 | 14.04.1996 | |
| 1156+295 | 4C29.45 | 132 | 140 | 173 | 2 2 | 08.07.1994 | |
| 1308+326 | AU CVn | 42 | 141 | 94 | 1 1 | 08.07.1994 | |
| 1611+343 | DA406 | 108 | 103 | 41 | 3 1 | 08.07.1994 | |
| 1633+382 | 4C38.41 | 102 | 219 | 224 | 3 1 | 12.04.1995 | |
| 1637+574 | OS562 | 110 | 173 | 117 | 2 1 | 11.01.1997 | |
| 1739+522 | 4C51.37 | 94 | 88 | 67 | 2 1 | 08.07.1994 | |
| 1803+784 | | 88 | 81 | 70 | 2 1 | 08.07.1994 | |
| 2234+282 | CTD135 | 110 | 242 | 177 | 2 1 | 08.07.1994 | |

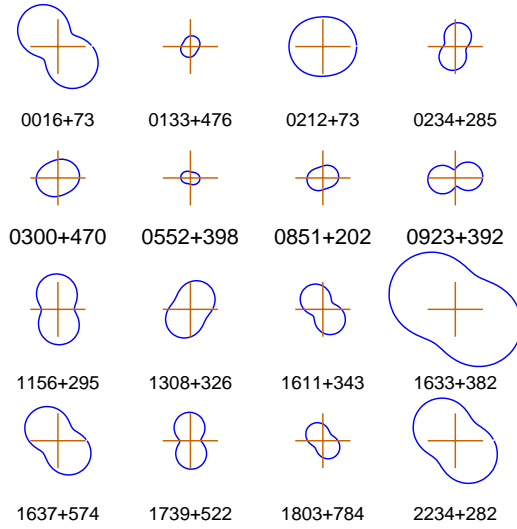
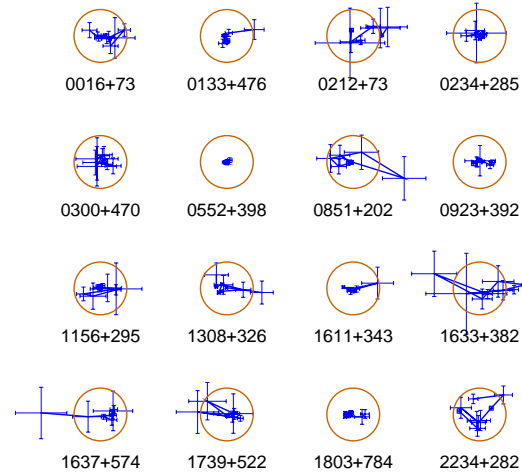
we further kept only sources north of +20 degrees in declination. A total of 16 sources passed successfully this double selection. They are listed in Table 2, together with information on the type of objects, redshift and flux density taken from Véron & Véron (1998), and the standard deviations of half-yearly positions with respect to the mean over the total time interval, in right ascension and declination.

3. Local astrometry

The VLBI results are expressed in the equatorial system of coordinates (right ascensions and declinations), which is linked to the Earth's rotation axis and has no particular relationship with the source geometry. On the other hand, most of the known activity of quasars takes the form of jets, i.e., aligned moving emissive structures that induce motions of the observed emission centre relative to a fixed background. We therefore considered for each source a local system of axes centered at the mean equatorial coordinates of the source for the whole observation span (1988-1999): the x-axis is in the direction of maximum standard deviation of the 0.5 year weighted averaged coordinates over 1988-1999, and the y-axis forms a direct rectangular system with it. Fig. 1 shows the ellipses of standard deviations of the 0.5 year averages, in the equatorial reference frame.

Note that there is no particular sign of a preferred N-S direction for the maximum standard deviation, suggesting that the contribution of the ill-modelled propagation delay due to the wet troposphere is not dominant in our sample of selected sources.

Table 3 gives, for the 16 sources under study, the directions of maximum variability (0 and 180 degrees correspond to the direction of right ascensions, 90 degrees to the direction of decli-

**Fig. 1.** Standard deviation of the 1988-1999 weighted mean positions at 0.5 year interval in equatorial coordinates. Abscissae: $\alpha\cos\delta$, ordinates: δ . The crosses show amplitudes of ± 0.25 mas.**Fig. 2.** Yearly weighted mean positions 1991-1999 in the source-fixed frames. Diameters of the circles: 0.5 mas

nations), and the standard deviations along the two source-fixed axes. For reference, Table 3 also gives the structure indices in X and S computed by Fey & Charlot (1997, 2000). These indices qualify the nuisance of the structure in astrometric positioning of the source. They range from 1 for very little disturbance through 4 for disrupting effect.

Fig. 2 shows the 2D source displacements (yearly values) of the same sources over 1991-1999 in the source-fixed frames. The error bars represent the standard error of the yearly averaged coordinates.

4. Statistical behaviour

The spectral characteristics of the time series of 0.5-year coordinates in the source-fixed frames are investigated using the Allan variance method (Allan 1966, see a review of these methods in Rutman 1978). The Allan variance analysis allows one to char-

Table 4. Source stability along maximum variance axis

| Source | Other Name | Variability at 0.5a | | Spectr. | Assumed distance Mpc |
|----------|------------|---------------------|------|---------|----------------------|
| | | μas | pc | | |
| 0016+731 | | 478 | 3.34 | White | 4002 |
| 0133+476 | DA55 | 115 | 0.80 | Flicker | 2668 |
| 0212+735 | | 105 | 0.69 | White | 4553 |
| 0234+285 | 4C28.07 | 59 | 0.42 | White | 3273 |
| 0300+470 | 4C47.08 | 59 | | White | |
| 0552+398 | OA198 | 139 | 0.91 | Flicker | 4553 |
| 0851+202 | OJ287 | 152 | 0.71 | White | 1263 |
| 0923+392 | 4C39.25 | 221 | 1.47 | White | 2330 |
| 1156+295 | 4C29.45 | 145 | 0.97 | White | 2397 |
| 1308+326 | AU CVn | 160 | 1.14 | White | 2929 |
| 1611+343 | DA406 | 162 | 1.16 | Flicker | 3545 |
| 1633+382 | 4C38.41 | 169 | 1.18 | Flicker | 4035 |
| 1637+574 | OS562 | 96 | 0.65 | Flicker | 2441 |
| 1739+522 | 4C51.37 | 196 | 1.41 | Flicker | 3518 |
| 1803+784 | | 135 | 0.89 | Flicker | 2285 |
| 2234+282 | CTD135 | 115 | 0.79 | White | 2546 |

acterize the power spectrum of the variabilities in time series, for sampling times ranging from the initial interval of the series to 1/4 to 1/3 of the data span, in our case 6 months to 3-4 years. This method identifies white noise (spectral density S independent of frequency f), flicker noise (S proportional to f^{-1}), and random walk (S proportional to f^{-2}), and it allows to specify the time frame in which a given type of noise is valid. Note that one can simulate flicker noise in a time series by introducing steps with a random amplitude at random dates. Fig. 3 gives the Allan variance graphs in the sources-fixed frames. In this log-log plot of the Allan variance as a function of sampling times (here 0.5, 1, 2, and 4 years), a slope equal to -1 is the signature of white noise, while a slope equal to zero is the signature of flicker noise. The blue/heavy stars plots are for the direction of the local x-axis, yellow/light open circles for the y-axis.

Most sources show similar stability signatures in both the x- and y-directions up to four years sampling time. Four sources, 1611+343, 1633+382, 1739+522, and 1803+784, show a remarkable discrepancy between flicker noise behaviour in the x-direction and marked white noise behaviour, at a much lower level, in the y-direction.

Considering the Standard Model (deceleration parameter $q_0=0.5$, cosmological constant $\Lambda=0$) and a value $H_0=60\text{km/s/Mpc}$ for the Hubble constant, one can compute distances of objects as a function of the redshift (Mattig 1958), and hence transform angular dimensions into linear ones (Theureau 2000). Table 4 summarizes the characterization of the sources stability in angular and linear units.

5. Conclusion

Using a small subset of the compact extragalactic radio sources that are monitored in at 13 cm and 3.6 cm in the framework of the maintenance of the International Celestial Reference Frame

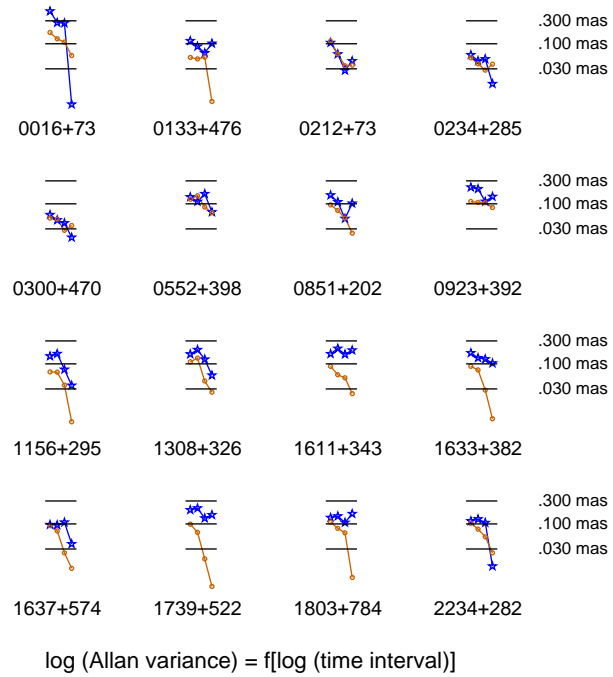


Fig. 3. Allan variance plot for sampling times ranging from 0.5 to 4 years over 1988-1999. Blue/heavy stars: direction of the local x-axis; yellow/light circles: y-axis

ICRF, we showed that detailed reliable position information can be derived since the late 1980's, with a 0.5 year resolution. The study is restricted to sources north of +20 degrees in declination, to avoid a possible contribution of the propagation delay due to the wet troposphere to the apparent stability in declination. The analysis shows that the time variability of these objects have varied spectral characteristics, that could possibly be related to diversified physical processes.

Acknowledgements. This research has made use of the US Naval Observatory (USNO) Radio Reference Frame Image Database (RRFID), of the Centre de Données Astronomiques de Strasbourg (CDS) and of NASA's Astrophysics Data System Abstract Service.

References

- Allan D.W., 1966, Proc. IEEE 54, 221.
- Charlot P., Sovers O.J., 1997, The New International Celestial Reference Frame, 23rd meeting of the IAU, Joint Discussion 7, 22 August 1997, Kyoto, Japan., 7, E6
- Feissel M., Mignard F., 1998, A&A 331, L33
- Fey A.L., Charlot P., 1997, ApJS 111, 95
- Fey A.L., Charlot P., 2000, ApJS, in press
- International Earth Rotation Service (IERS), 1999, 1998 Annual Report, 83, Observatoire de Paris
- Ma C., Arias E.F., Eubanks T.M., et al., 1998, AJ 116, 516
- Mattig W., 1958, Astron. Nachr. 284, 109
- Rutman J., 1978, Proc. IEEE 66, 1048
- Sovers O.J., Fenselow J.L., Jacobs C.S., 1998, Reviews of Modern Physics 70, 1393
- Theureau G., 2000, Private communication
- Véron-Cetty M.-P., Véron P., 1998, A Catalogue of quasars and active nuclei, 8th ed., ESO Scientific Report Series 18. Garching: European Southern Observatory (ESO)